

Supplementary Materials:

1. Microchannel device design

Seven different microfluidic devices as shown in Figure S1 were designed using commercially available SolidWorks software. Each device has three parts: an inlet area, a working area, and an outlet area. Among them, the variation is the working area. The proposed seven devices can be categorized into two groups: single-layer decrement and symmetric double-layer decrement. Design concepts for each individual device are described below.

Type 1: Single-layer decrement microchannels: Decrement microchannels allow the cell suspension to flow from larger microchannels to relatively smaller microchannels, progressively damaging cell membranes.

Type 2: Symmetric double-layer decrement microchannels: The first layer enables progressive damage of cell membranes and the incrementally increasing channel size of the second layer allows the liquid to be easily taken out and collected.

Type 3: Symmetric double-layer decrement device with enlarged: microchannels at the outlet Elongated length and incrementally increasing channel size at the outlet of the second layer facilitates the liquid to flow out along with the enlarged microchannels.

Type 4: Single-layer decrement device with enlarged microchannels at the outlet: Single-layer decrement structure has enlarged microchannels at the outlet.

Type 5: Parallel arranged cylinders: Parallel arranged $\phi 100\ \mu\text{m}$ cylinders with the gap between two cylinders.

Type 6: Parallel arranged rectangular columns: Parallel arranged rectangular columns having length of $250\ \mu\text{m}$ and the gap between two neighboring columns of $5\ \mu\text{m}$.

Type 7: Parallel arranged columns with rhombus shape at both end: Parallel arranged columns with rhombus shape at both ends and the gap between two neighboring columns of $5\ \mu\text{m}$. The rhombus shape allows the cells to be easily dispersed into the device.

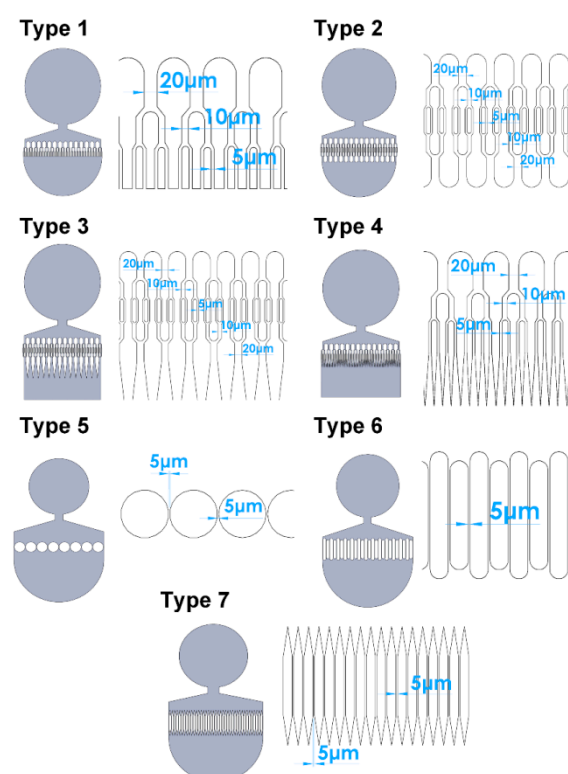


Figure S1. Seven different microfluidic devices

2. Fabrication of silicon based replica molds

The optical microscopy images of the fabricated silicon base replica molds of the designed microchannel devices with photoresist as the structure are shown in Figure S2. The results indicate that all the designed

microchannel structures could be successfully transferred to photoresist. The silicon base replica molds could be further implemented for PDMS casting.

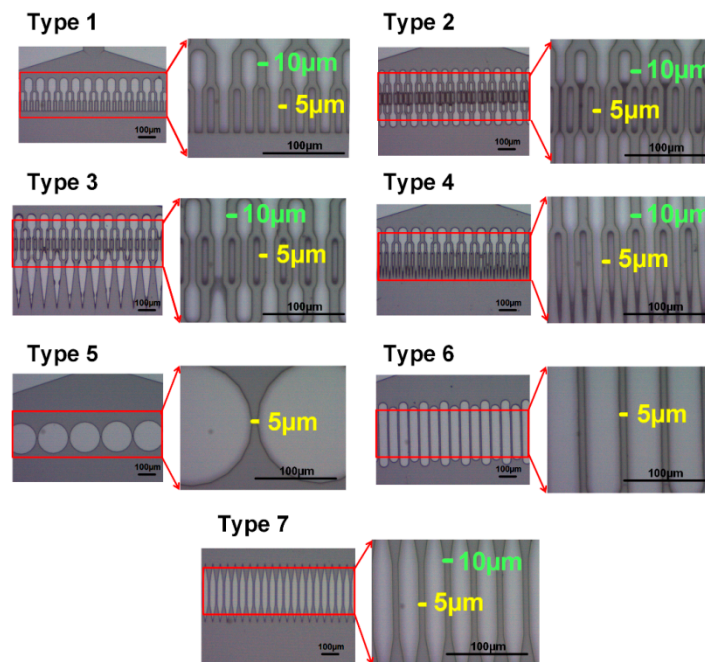


Figure S2. The optical microscopy images of the fabricated silicon base replica molds of the designed microchannel devices with photoresist as the structure

3. PDMS casting

The optical microscopy images of the PDMS based microchannel structures obtained by casting PDMS solutions on the silicon base replica molds are depicted in Figure S3. We can observe that the designed patterns could be completely copied to PDMS.

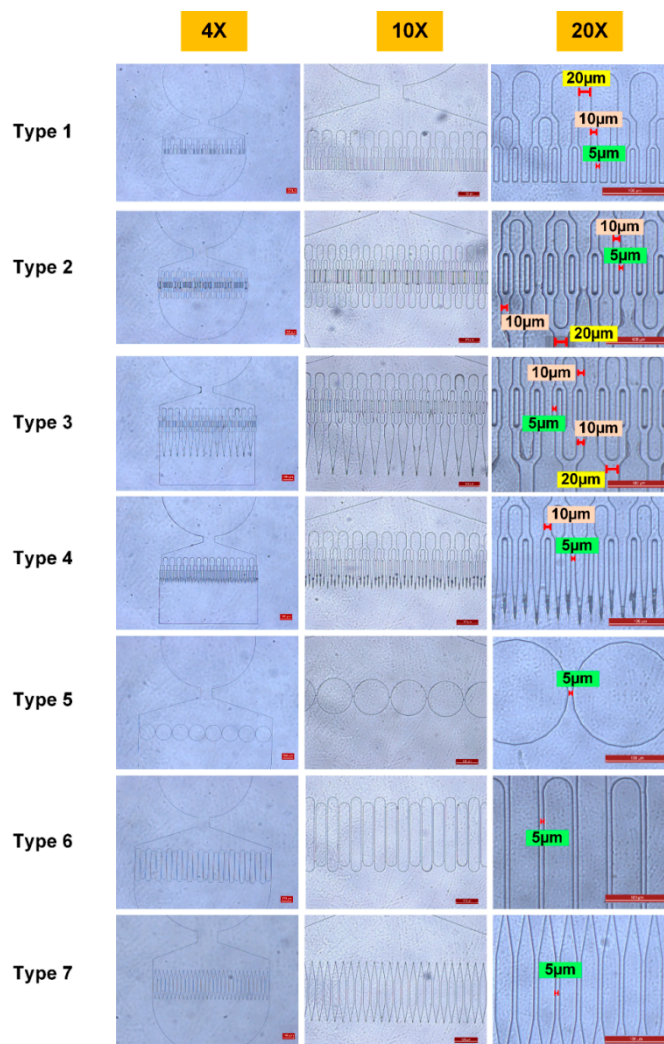


Figure S3. The optical microscopy images of the PDMS based microchannel structures obtained by casting PDMS solutions on the silicon base replica molds

4. Cell lysis ability of the fabricated microfluidic devices

Figure S4 shows the images of the cell lysis process. The first column presents the images when the cell suspensions were initially injected. As shown in the second column, cells were broken when passed through the 5 μm microchannels, releasing cytoplasm, nucleus and membrane fragments. Undamaged cells at the inlet area are indicated by red arrows. It can be found that cells easily congregated and blocked the front end of the working areas in type 5 and 6 devices, as indicated by the yellow circles. As the released substances in the microchannels were increasingly accumulated, the viscosity of the suspension at the outlet area increased, hence further blocked the outlet of the working area. For the type 1-4 devices (decrement microchannel structures), the outlet areas were heavily blocked by the released substances, even though cells could be effectively broken. For the type 7 device, not much blocking was found whether in the inlet, working, and blocking areas. Zygomorphic streamline clusters and pressure distribution and symmetrical velocity distribution enable the cell suspension to uniformly pass through the microchannels and effectively damaged cells.

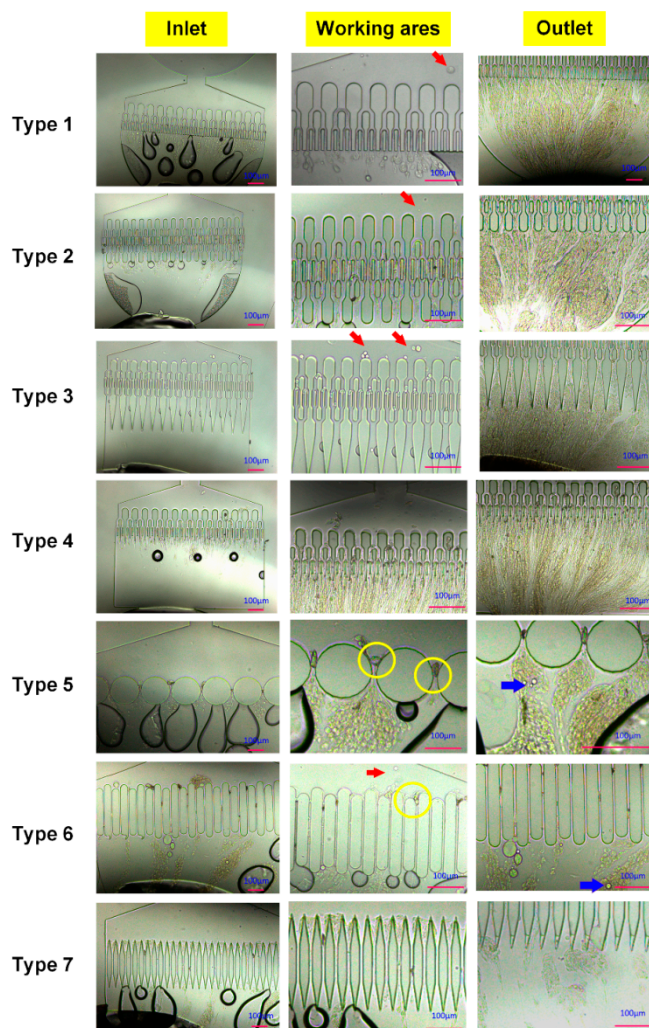


Figure S4. The optical microscopy images of the cell lysis process using chip-based microfluidic device. Arrows indicate the cell particles without damage. Circles indicate the cell congregation in the front of working area.

5. Effectively usable time

Serious obstruction and unbalancing pressure induced device damage will terminate the cell lysis function of a device. The effectively usable time of a device is defined as when either no suspension can be collected at the outlet area or unbalancing pressure induced damage occurs. A longer usable time implies more collections of suspension at the outlet area. Table S1 tabulates the effectively usable time of these seven devices. The type 7 device has a relatively longer usable time.

Table S1. Effectively usable time of the designed devices

Device type	1	2	3	4	5	6	7
Usable time (min)	25	13.5	12	18.5	18	27.3	29.3

6. Optimal microchannel device

Considering the cell lysis capability, fluidity of the suspension at working area, and effectively usable time, the type 7 device was selected as the desired device for further experiments.